LCLS-II-HE Undulator Beam Pipe Corrector Calibration

Zachary Wolf, Yurii Levashov
Stanford Linear Accelerator Center

June 8, 2023

Abstract

The LCLS-II-HE project will upgrade the soft x-ray line with longer period undulators. The new period requires a new calibration of the beam pipe correctors. This note documents the new soft x-ray undulator beam pipe corrector calibration.

1 Introduction[1]

The beam trajectories in the LCLS-II-HE undulators are tuned in the laboratory to be straight at all gaps. When the undulator is placed in the undulator hall tunnel in a different background magnetic field, the trajectories become curved, reducing the undulator performance. Correction coils have been built into the beam pipe to mitigate this problem. The current required in the correction coils depends on the magnitude and direction of the difference in the background magnetic field between the tunnel and the lab, and the current also depends on the undulator gap. The magnetic field in the tunnel has been mapped, so the difference in background fields is known. In the lab this difference is simulated by a large Helmholtz coil. The effect of the field difference must be determined as a function of undulator gap, and the current in the trim windings to correct the difference must be determined.

The beam pipe correctors were calibrated for the LCLS-II project for both the soft x-ray (SXR) and hard x-ray (HXR) lines and the results are documented in a technical note[2] referred to in what follows by giving only the note number LCLS-TN-20-2. For the LCLS-II-HE project, the SXR undulator (SXU) period is increased from 39 to 56 mm. This necessitates a new calibration of the SXU beam pipe correctors. We performed the calibration for one representative HE-SXR undulator and assume the calibration applies to all HE-SXR undulators because of their similarity. The results of the calibration are the subject of this note.

The measurements took place in the spring of 2023. The HE-SXR undulator used for the test was HE-SXU-000.

[1] Work supported in part by the DOE Contract DE-AC02-76SF00515. This work was performed in support of the LCLS project at SLAC.

[2] Z. Wolf and Y. Levashov, "LCLS-II Undulator Beam Pipe Corrector Calibration", LCLS-TN-20-2, June, 2020.

2 Undulator Tuning Requirements

In order to discuss the relevance of the effect of changes in the background magnetic fields, we must know how the field difference affects the undulator parameters relative to the tolerances on the parameters. The LCLS-II-HE undulator tolerances come from an undulator Physics Requirements Document.[3] The list of requirements relevant to this note are briefly summarized below.

2.1 HE-SXU Requirements

1. The minimum operational K value is $K_{\min} = 1.51$, and the maximum K value at the minimum operational gap of 7.2 mm is $K_{\max} > 9.21$. The K value must be known to $\pm 5.5 \times 10^{-4}$ at all gap settings.

2. The total phase advance in the 4.40000 meter long cell must be known to ± 10 degrees.

3. The first field integral of B_x and B_y must be within $\pm 50 \times 10^{-6}$ Tm of zero. The second field integral of B_x and B_y must within $\pm 200 \times 10^{-6}$ Tm^2 of zero.

3 Effect Of The Background Field Difference

As noted in the introduction, the beam trajectories in the undulators are tuned to be straight in the Magnetic Measurement Facility (MMF). This is done in the presence of the background magnetic field in the MMF. When the undulators are moved to the undulator hall tunnel, the background magnetic field is different. The extra field causes the beam to follow a curved path through the undulator. In this section we estimate the consequences of the curved trajectory. Only the results of calculations are presented. The details of the calculations can be found in technical note LCLS-TN-20-2 referenced above. Estimates are made in order to determine the accuracy with which we need to correct the background fields.

Consider an HE-SXR undulator with an additional constant field $\overrightarrow{b}_0$ in the y-direction on the beam axis. The additional field causes a curvature to the beam trajectory. This in turn causes a relative change in the K value given by

$$\frac{\delta K}{K} = \frac{1}{12K^2}\left(\frac{e}{mc}b_0\right)^2 L^2 \tag{1}$$

where e is the electron charge, m is the electron mass, c is the speed of light, and L is the undulator length. The relative change in K due to the trajectory curvature becomes large at small K. If we assume $K = 1.51$, the minimum K value of the operating range, and we use the length of the undulator $L = 3.4$ m, we get the relative change in K as a function of uncorrected external field b_0 shown in figure 1. The tolerance is $\delta K/K = 5.5 \times 10^{-4}$. With the long period HE-SXR undulators, it appears that external uncorrected fields will not exceed the K tolerance, but may use a significant fraction of the tolerance if the field differences are large.

[3] D. Cesar et al., "LCLS-II-HE SXR Undulator System", Physics Requirements Document LCLSII-HE-1.3-PR-0049-R0.

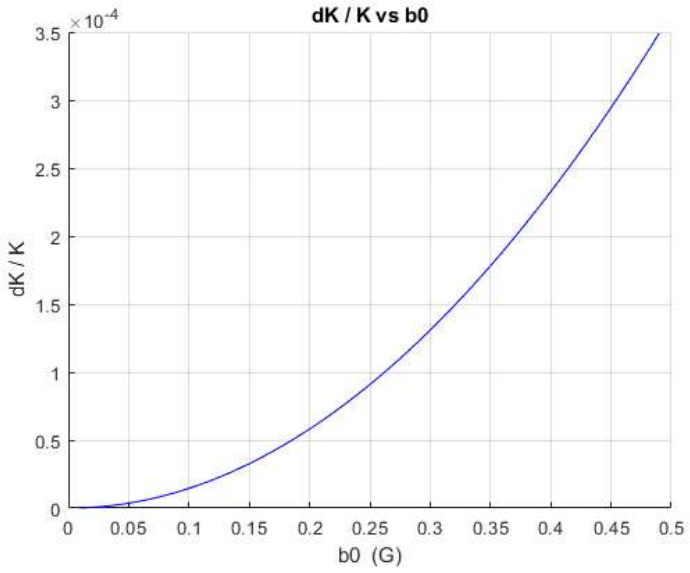

Figure 1: $\delta K/K$ as a function of uncorrected field b_0 using $K_{\min} = 1.51$.

The phase advance through the cell is affected by the additional path length of the curved trajectory. The change in cell phase from the added trajectory curvature is

$$\delta\Phi = \frac{\pi}{6\lambda_u\left(1+\frac{1}{2}K^2\right)}\left(\frac{e}{mc}b_0\right)^2 L^3 \tag{2}$$

The smaller the K value, the larger the change in cell phase. In figure 2 we plot the change in cell phase as a function of uncorrected external field strength. The uncorrected external fields do not exceed the 10 deg tolerance on knowing the cell phase, but they use a significant fraction of the tolerance at large field differences.

Uncorrected changes in the external fields have the largest effect on the field integrals. In particular, on the integrals of B_y. There is an enhancement in an applied B_y as the undulator gap is closed. This is due to the external field concentrating in the steel poles as the field takes the lowest reluctance path. The field enhancement is demonstrated in figure 3. An external field of 0.3 G was applied to HE-SXU-000 using a large Helmholtz coil described below. The field integrals were measured at different gaps, and the Earth field with no field from the Helmholtz coil was subtracted. The first integral of B_y increased by a factor of 2.2 as the gap went from 180 mm to 7.2 mm. The same result was obtained when an external field of -0.3 G was applied. We need to include this enhancement factor when calculating the effect on field integrals due to uncorrected changes in background fields. For completeness, we show the effect of applying an external B_x field in figure 4. In this case, the lowest reluctance path is through the steel poles instead of through the gap, making the B_x field integrals small at small undulator gaps.

The change to the first integral of B_y, I_{1y}, is proportional to the uncorrected external field b_0 and to the undulator length L.

$$I_{1y} = 2.2 b_0 L \tag{3}$$

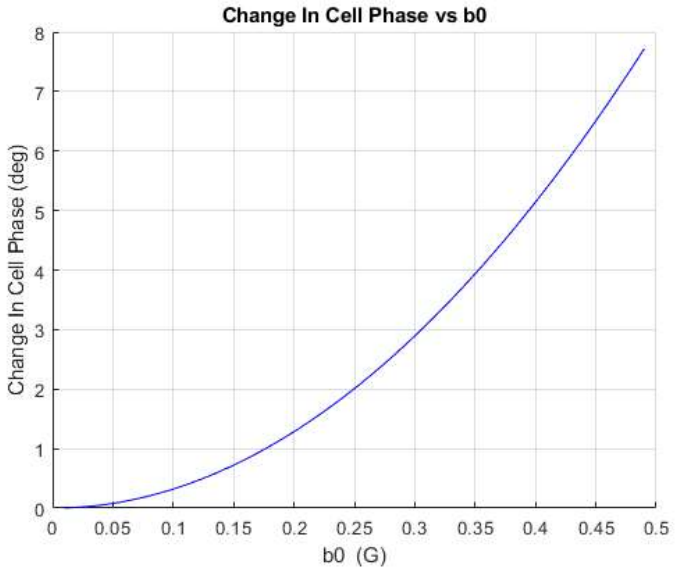

Figure 2: Change in cell phase as a function of uncorrected field b_0 using $K_{\min} = 1.51$.

The enhancement factor of 2.2 is included. Figure 5 shows the change in first field integral as a function of the uncorrected external field. The tolerance of 50 μTm is exceeded if the uncorrected external field exceeds 0.067 G. This is the most strict requirement for the beam pipe corrector calibration accuracy.

The change to the second integral of B_y, I_{2y}, is proportional to the field enhancement factor of 2.2, the uncorrected external field b_0, and to the undulator length L squared.

$$I_{1y} = 2.2\frac{1}{2}b_0 L^2 \tag{4}$$

Figure 6 shows the change in second field integral as a function of the uncorrected external field. The tolerance of 200 μTm^2 is exceeded if the uncorrected external field exceeds 0.157 G.

In summary, an external field difference between the MMF and the tunnel must be corrected by the beam pipe corrector to better than 0.067 G in order to meet the physics requirements.

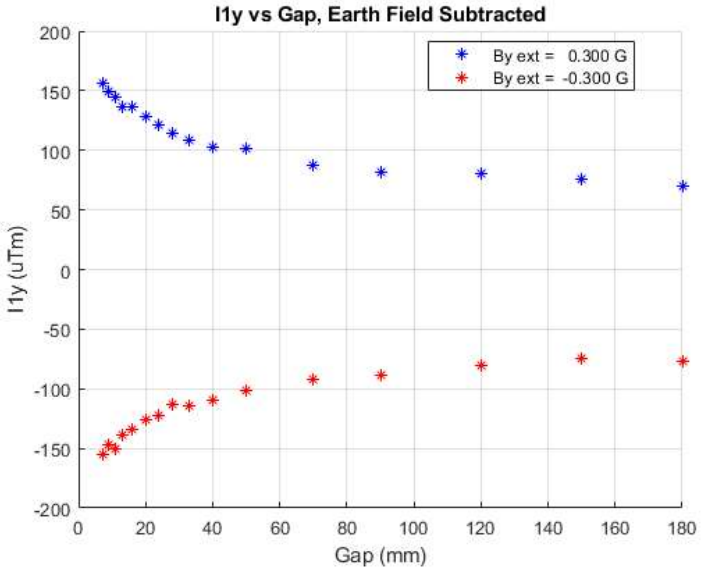

Figure 3: An external B_y field is enhanced by a factor of 2.2 as the undulator gap is closed.

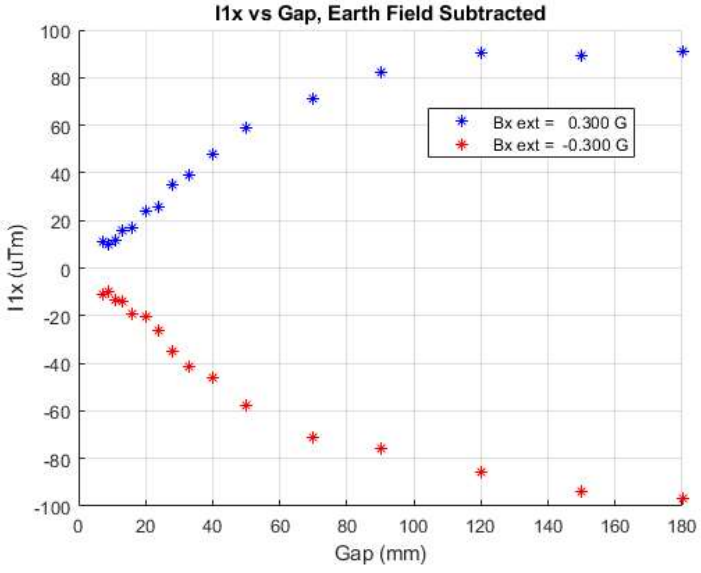

Figure 4: At small gap, an external B_x field is shunted around the undulator gap by the steel poles.

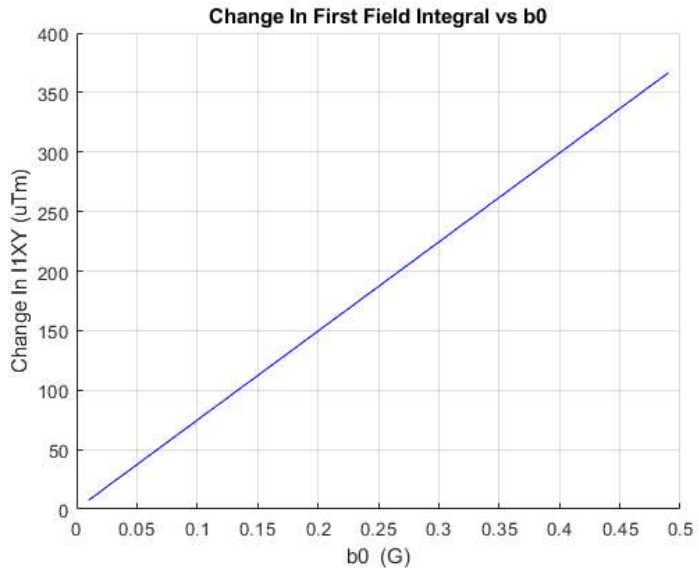

Figure 5: Change in first field integral as a function of uncorrected external field.

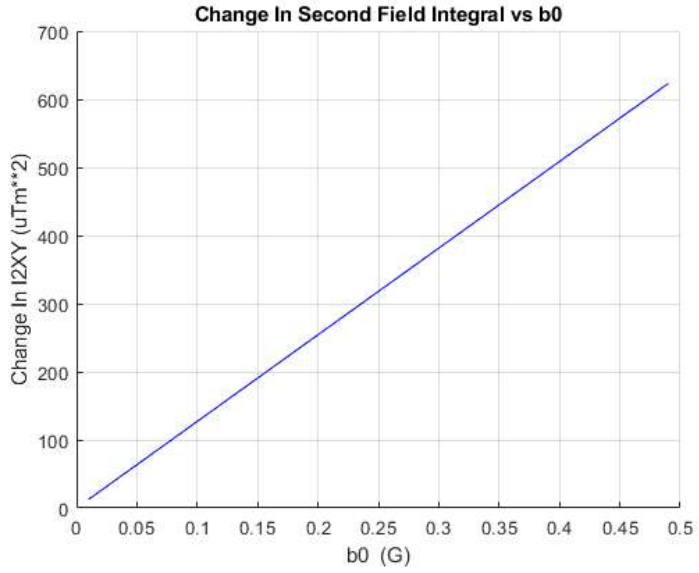

Figure 6: Change in second field integral as a function of uncorrected external field.

4 Field Differences Between The Tunnel And The Laboratory

The magnetic fields in the laboratory and in the tunnel have been mapped.[4] The background fields measured at the SXR undulator bench in the MMF are shown in figure 7.

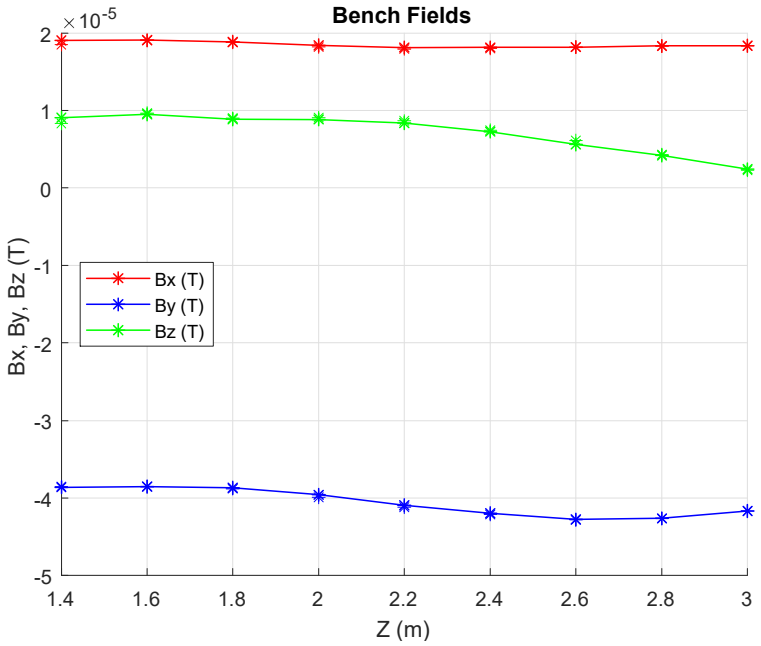

Figure 7: Field measurements at the SXR undulator bench.

The background fields in the tunnel at the locations of the SXR undulators are shown in figure 8. The difference in the fields is shown in figure 9. Differences up to 0.18 G are evident.

[4] S. Anderson, "Earth's Field Measurements For The LCLS-II Undulator Lines And MMF Benches", April, 2020.

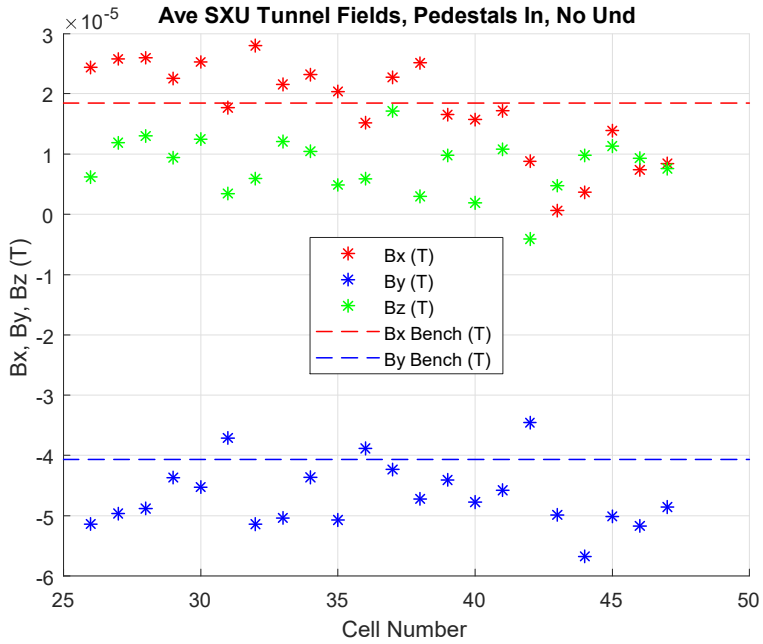

Figure 8: Measured magnetic field in the tunnel and at the measurement benches for the SXR undulators.

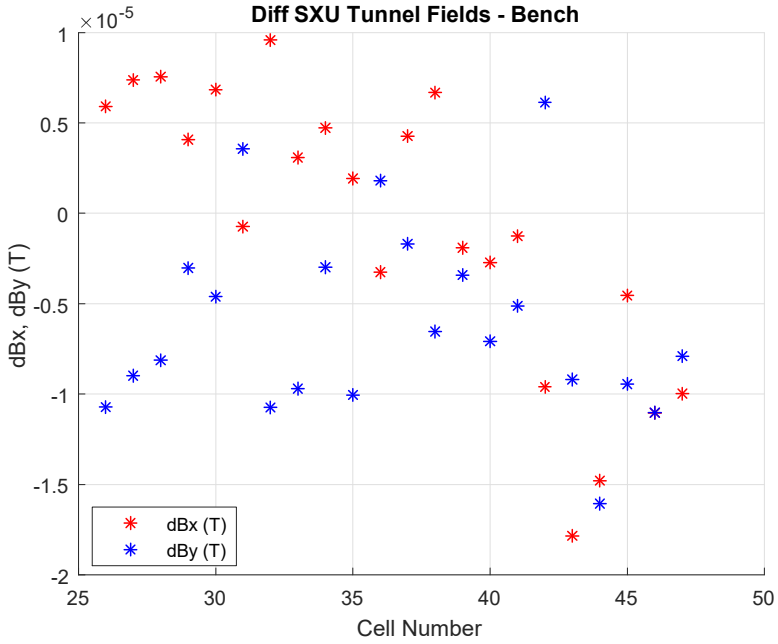

Figure 9: Field difference between the tunnel and the measurement bench for the SXR undulators.

5 Measurement Setup

In order to measure the effect of an external field on an undulator, we need to apply an external field in the measurement laboratory. We do this using a large Helmholtz coil. The Helmholtz coil surrounds the undulator, which has a beam pipe with correction coils inside it. The field inside the beam pipe is measured with a stretched wire system which gives the first and second integrals of B_x and B_y.

5.1 Helmholtz Coil

A large Helmholtz coil was used to make changes to the background field of the undulator. Figure 10 shows the Helmholtz coil assembled around HE-SXU-000 and its measurement bench. Figure 11 shows the power supplies for the Helmholtz coil and the beam pipe

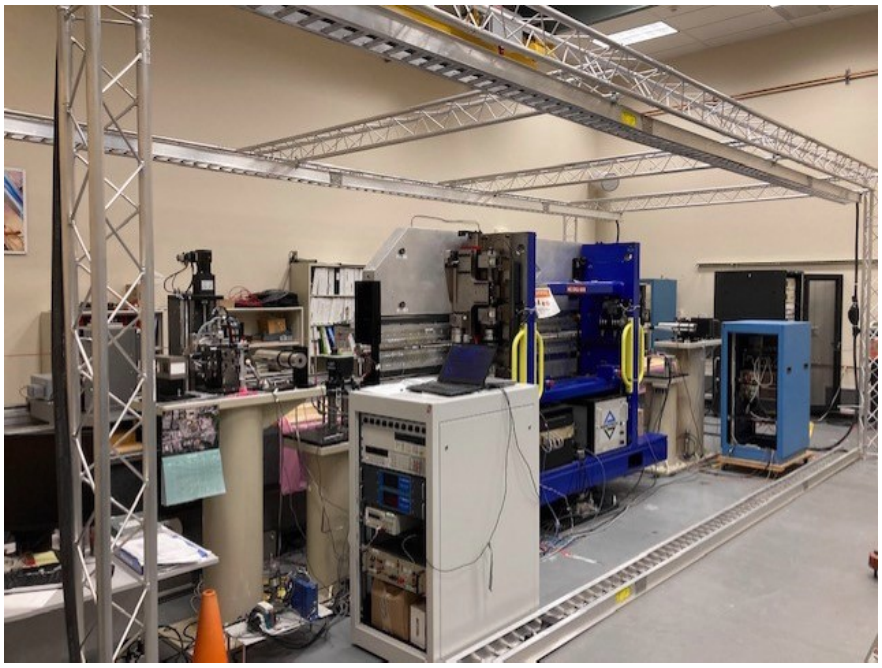

Figure 10: A large Helmholtz coil is used to make changes to the background field of HE-SXU-000.

correctors. The beam height is roughly 1.4 m above the floor. This sets the size of the Helmholtz coil. The cables in the coil are placed in a square 2.8 m on a side centered on the beam line. A diagram of the setup is shown in figure 12.

Two power supplies are used to generate a magnetic field up to 0.5 G in any direction. The wiring diagram is illustrated in figure 13. The polarities of the currents in the windings are given in figure 14. The coils are wired so that coil 1 produces a field in the +x, +y (quadrant 1) direction. Coil 2 produces a field in the -x, +y (quadrant 2) direction. The coil currents I_1 and I_2 are combined with the same magnitude but opposite sign to give I_x which produces a B_x field, and with the same magnitude and same sign to give I_y which

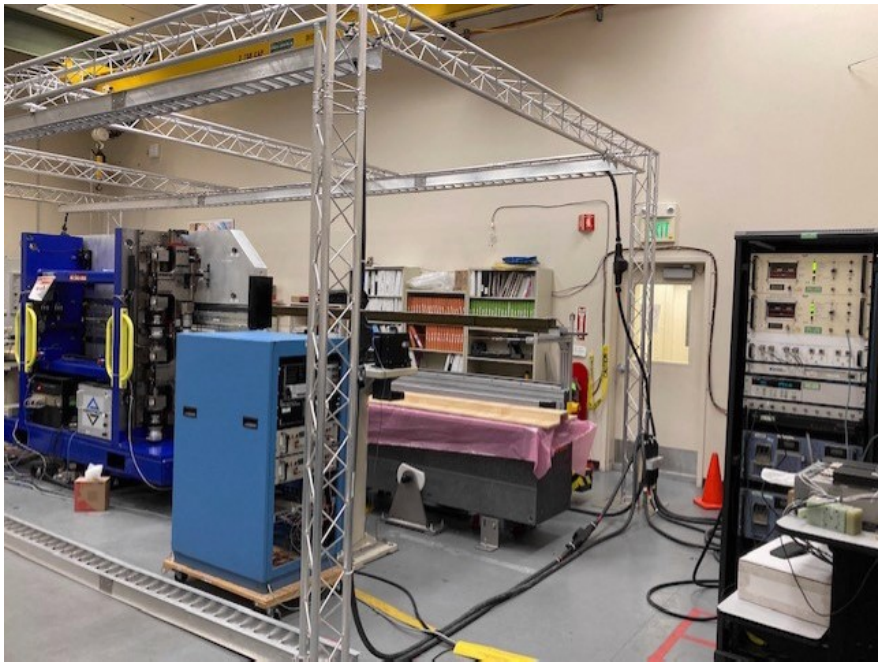

Figure 11: The Helmholtz coil is powered with the large supplies in the rack on the right. The beam pipe correctors are powered with the small supplies in the blue rack.

produces a B_y field. The relations between the currents and the fields are shown in the figure. The coordinate system has +z in the beam direction, +y up, and +x makes a right handed system.

The simple geometry makes it easy to calculate the field from the Helmholtz coil. For the current configuration in the figure which makes a B_x field, the field strength is given by

$$B_x = \frac{\mu_0 I}{2\pi r}\frac{1}{\sqrt{2}}4 \tag{5}$$

where $r = (d/2)\sqrt{2}$ and d is the 2.8 m width of the coil. The factor $1/\sqrt{2}$ comes from the field from each conductor being at 45 degrees with respect to the horizontal. The factor of 4 comes from the four conductors. Putting in numbers, and realizing that B_y behaves in the same way, we find

$$B_x = 0.2857 \text{ G / } 100 \text{ A} \tag{6}$$
$$B_y = 0.2857 \text{ G / } 100 \text{ A} \tag{7}$$

where the 100 A is the current I_x or I_y indicated in the wiring diagram.

The field from the Helmholtz coil with no undulator was modeled. With $I_x = 100$ A producing a B_x field in an infinitely long coil in z, the uniformity of B_x vs x at $y = 0$ is shown in figure 15. The field is uniform at the 5% level over $x = \pm 0.5$ m. The uniformity of B_x vs y at $x = 0$ is shown in figure 16.

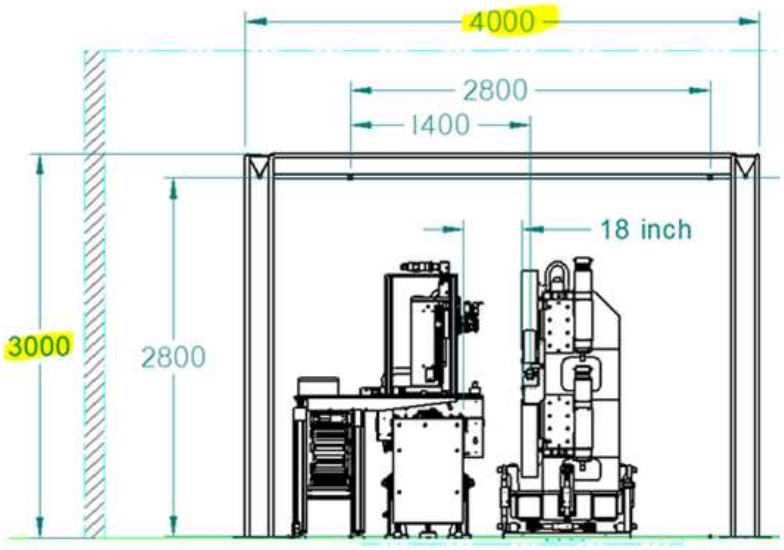

Figure 12: Diagram of the Helmholtz coil around the SXR Kugler bench. Dimensions are in mm.

The Helmholtz coil was originally assembled in a storage area. A map of the B_x field uniformity in the z-direction was made. The map with $I_x = 200$ A is shown in figure 17. The field is uniform over the 3.4 meter length of the undulators. For this configuration, the cables went straight down the supports at the end of the Helmholtz coil. We also tried configuring the cables in an "X" shape at the ends. This gave large fields on the beam axis at the ends. The configuration with the cables going down the supports was chosen as the more favorable.

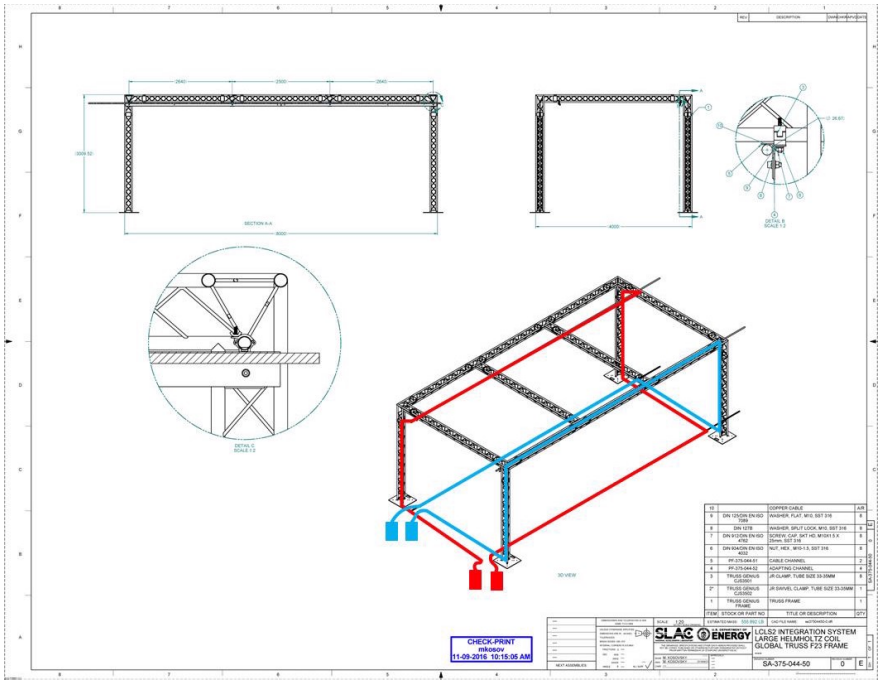

Figure 13: Wiring diagram for the Helmholtz coil.

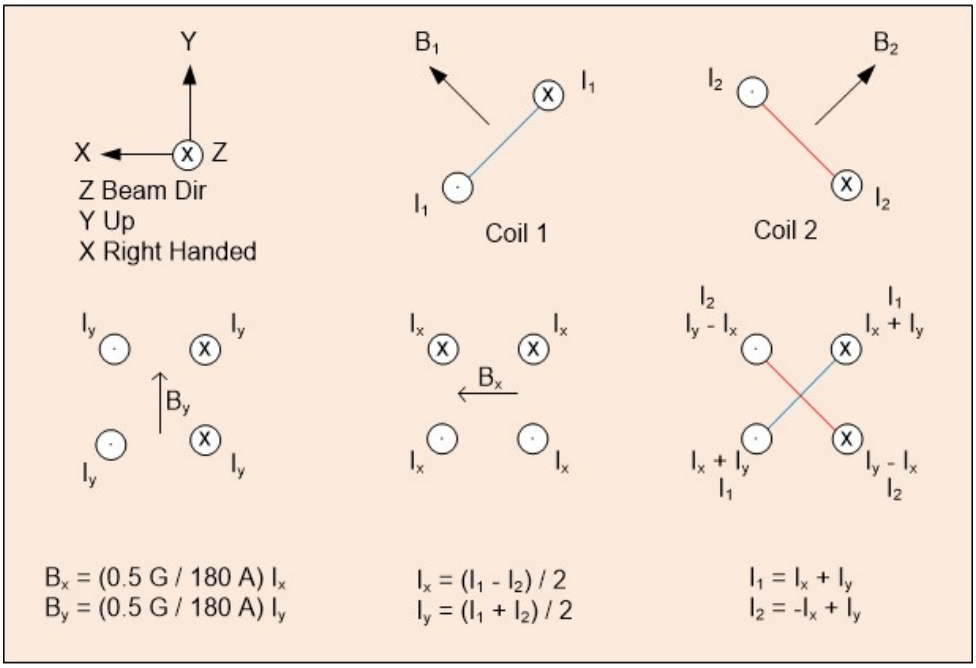

Figure 14: Polarity of the currents in the windings. The measured field in the Helmholtz coil for given current is indicated.

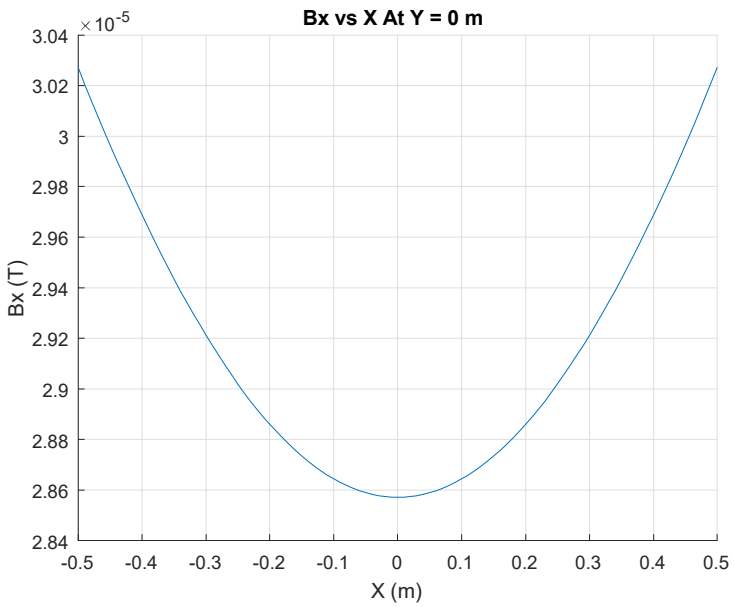

Figure 15: B_x vs x with $I_x = 100$ A.

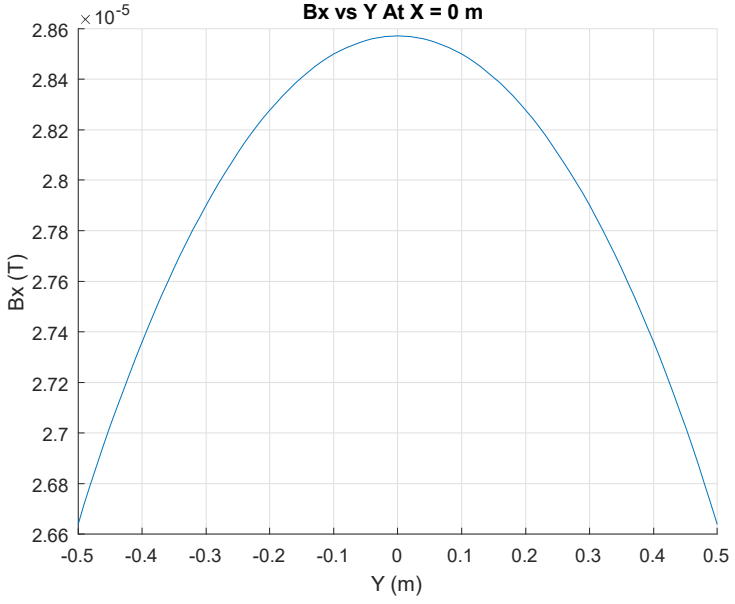

Figure 16: B_x vs y with $I_x = 100$ A.

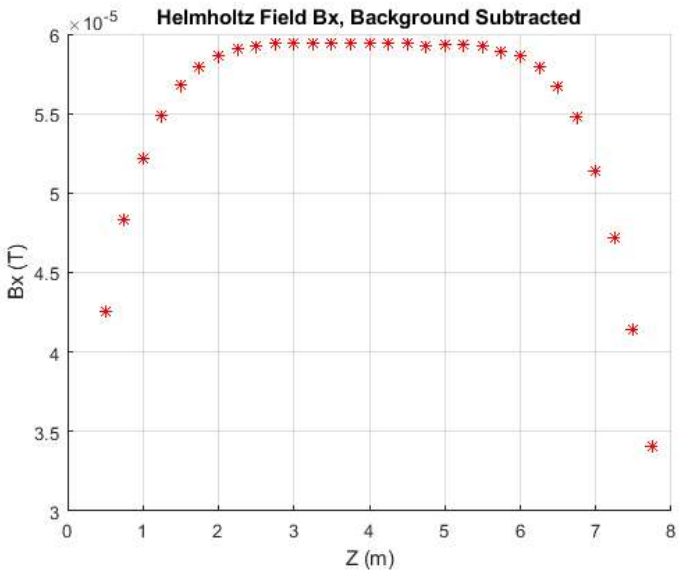

Figure 17: B_x vs z at $x = 0$ and $y = 0$ with $I_x = 200$ A.

5.2 Beam Pipe Corrector

The SXU beam pipe has a rectangular array of windings in a manner similar to the Helmholtz coil. Figure 18 shows a drawing of the HXR undulator beam pipe and figure 19 shows a photo.[5] The SXR beam pipe which we used for the calibration is very similar but has a horizontal orientation.

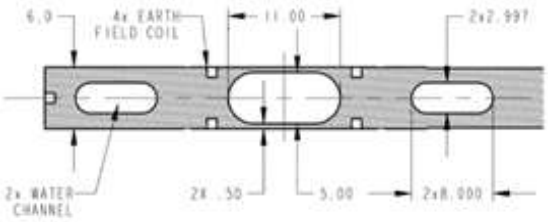

Figure 18: Drawing of the HXR undulator beam pipe.

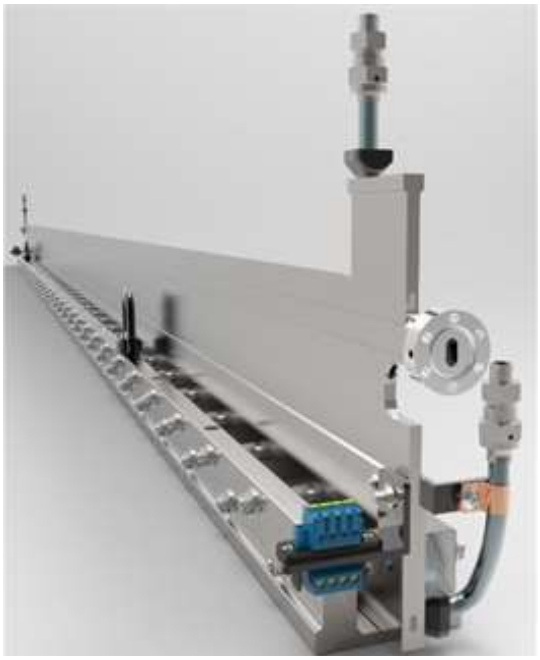

Figure 19: Photo of the HXR undulator beam pipe.

The beam pipe corrector coils for the SXR undulators are placed with the wire centers on a rectangular grid 14.5 mm by 5.0 mm. The diagonal wires are connected so that they produce two coils. A wiring diagram for the coils is shown in figure 20. The coils are

[5] J. Lerch, et al, "Design Of the HGVPU Undulator Vacuum Chamber For LCLS-II", Proceedings of NAPAC2016, Chicago, IL.

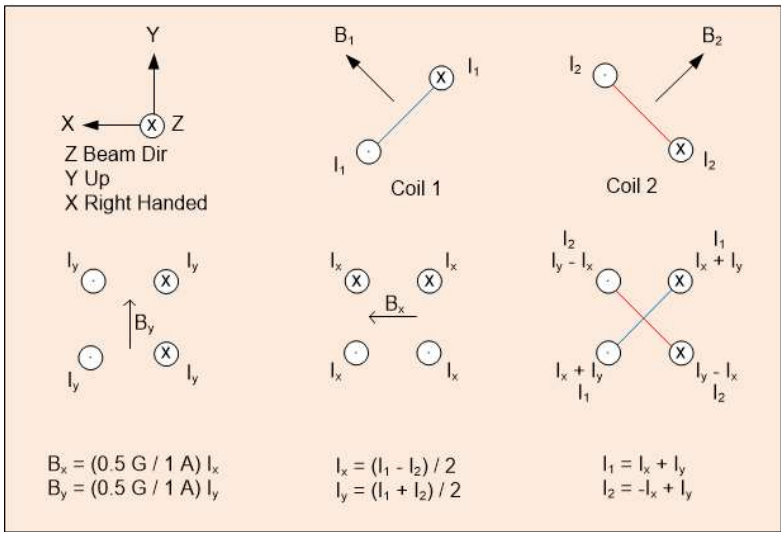

Figure 20: Wiring diagram for the beam pipe correctors.

wired so that coil 1 produces a field in the +x, +y (quadrant 1) direction. Coil 2 produces a field in the -x, +y (quadrant 2) direction. The coil currents I_1 and I_2 are combined with the same magnitude but opposite sign to give I_x which produces a B_x field, and with the same magnitude and same sign to give I_y which produces a B_y field. The relations between the currents and the fields are shown in the figure. The coordinate system has +z in the beam direction, +y up, and +x makes a right handed system. The transfer functions given in the figure are meant to only give an order of magnitude estimate. The actual transfer functions are gap dependent. The gap dependence of the fields was simulated. The gap dependence is due to the effect of the steel poles and can be understood using the associated image currents to model the steel. Details are given in LCLS-TN-20-2.

With no steel poles, the SXR beam pipe corrector transfer function is

$$B_x = 0.3401 \text{ G} / 1 \text{ A} \quad (8)$$

$$B_y = 0.9862 \text{ G} / 1 \text{ A} \quad (9)$$

The measurements should approach these values at large gaps.

6 Test Plan

6.1 Measure The Effect Of An External Applied Field

The measured difference in the background fields between the tunnel and the laboratory was discussed above. Field differences up to $\sim$ 0.18 G are present. Based on these measurements, we set the range of background field differences for these tests from -0.3 G to $+0.3$ G. We must also study the gap dependence of the effects of the external fields. The test plan is as follows:

1. Assemble the Helmholtz coil around the test bench and undulator.
2. Install a stretched wire measurement system with the stretched wire in the beam pipe. The beam pipe contains the trim windings.
3. Align the system so the trim windings and stretched wire are centered on the beam axis.
4. Define a set of undulator gaps to perform measurements at. For the HE-SXR undulators, measure at gaps of 7.2, 9, 11, 13, 16, 20, 24, 28, 33, 40, 50, 70, 90, 120, 150, 180 mm.
5. Define a set of measurements to perform at each undulator gap. For the HE-SXR undulators, measure the field integrals I_{1x}, I_{1y} at each undulator gap using the stretched wire system.
6. With no current in the Helmholtz coil, measure the field integrals at the undulator gaps.
7. Using the Helmholtz coil, apply a B_x field of 0.3 G. Measure the field integrals at a gap of 10 mm. Verify that the B_y field integrals do not change.
8. Using the Helmholtz coil, apply a B_y field of 0.3 G. Measure the field integrals at a gap of 10 mm. Verify that the B_x field integrals do not change.
9. Using the Helmholtz coil, apply B_x fields of -0.3, -0.2, -0.1, 0.0, 0.1, 0.2, 0.3 G. Measure the field integrals at the undulator gaps.
10. Using the Helmholtz coil, apply B_y fields of -0.3, -0.2, -0.1, 0.0, 0.1, 0.2, 0.3 G. Measure the field integrals at the undulator gaps.
11. Analyze the measurements to verify that the field integral variation depends linearly on the applied field at each undulator gap. Determine the two response coefficients dI_{1x}/dB_x and dI_{1y}/dB_y at each undulator gap.
12. Perform a spline fit to the gap dependence of the field integral response coefficients. Make a file of spline points fitting dI_{1x}/dB_x vs gap, and the same for dI_{1y}/dB_y vs gap.

6.2 Measure The Response Of The Beam Pipe Correctors

Determine how the beam pipe correctors behave at different undulator gaps. The measurement plan to do this is as follows:

1. Turn off the Helmholtz coil so no additional external fields are applied.
2. Define a set of undulator gaps to perform measurements at. For the HE-SXR undulators, measure at gaps of 7.2, 9, 11, 13, 16, 20, 24, 28, 33, 40, 50, 70, 90, 120, 150, 180 mm.
3. Define a set of measurements to perform at each undulator gap. For the HE-SXR undulators, measure the field integrals I_{1x}, I_{1y} at each undulator gap using the stretched wire system.
4. Apply a current of 1 Amp making a B_x field in the beam pipe corrector with an undulator gap of 10 mm. Verify that the B_y field integrals do not change.
5. Apply a current of 1 Amp making a B_y field in the beam pipe corrector with an undulator gap of 10 mm. Verify that the B_x field integrals do not change.
6. Apply currents of $I_x = -1.0, -0.5, 0.0, 0.5, 1.0$ A making a B_x field in the beam pipe corrector. Measure the field integrals at the undulator gaps.
7. Apply currents of $I_y = -1.0, -0.5, 0.0, 0.5, 1.0$ A making a B_y field in the beam pipe corrector. Measure the field integrals at the undulator gaps.
8. Analyze the measurements to verify that the field integrals vary linearly with the applied current at each undulator gap. Determine the two response coefficients dI_{1x}/dI_x and dI_{1y}/dI_y at each undulator gap.
9. Perform a spline fit to the gap dependence of the field integral response coefficients. Make a file of spline points fitting dI_{1x}/dI_x vs gap, and the same for dI_{1y}/dI_y vs gap.

6.3 Calibrate The Beam Pipe Correctors

In the following sections the symbols used for currents are I_x and I_y. The symbols used for first field integrals are I_{1x} and I_{1y}. The context and units should prevent confusion, but the similarity of the symbols must be noted.

At this point, the change in undulator field integral for a given external applied field is known. These are the fits to dI_{1x}/dB_x and dI_{1y}/dB_y as a function of gap. For a given field difference between the tunnel and the lab ΔB, the response parameter times the field difference gives the change in the undulator field integral at a given undulator gap g.

$$\Delta I_{1x}(g) = \frac{dI_{1x}}{dB_x}(g)\ \Delta B_x \tag{10}$$

$$\Delta I_{1y}(g) = \frac{dI_{1y}}{dB_y}(g)\ \Delta B_y \tag{11}$$

We also know the change in undulator field integral for a given current in the beam pipe corrector windings as a function of undulator gap. These are the fits to dI_{1x}/dI_x and dI_{1y}/dI_y as a function of gap. For a given current I_x or I_y, the response parameter times the current gives the change in the undulator field integral at a given undulator gap g.

$$\Delta I_{1x}(g) = \frac{dI_{1x}}{dI_x}(g)\ I_x \tag{12}$$

$$\Delta I_{1y}(g) = \frac{dI_{1y}}{dI_y}(g)\ I_y \tag{13}$$

Combining these results, for given external field difference between the tunnel and the lab, we know the change in the undulator field integrals. We can set the trim current to give the negative of the change of the undulator field integral. In this way, the field integral has the same value it had in the lab during calibration.

$$\frac{dI_{1x}}{dI_x}(g)\ I_x = -\frac{dI_{1x}}{dB_x}(g)\ \Delta B_x \tag{14}$$

$$\frac{dI_{1y}}{dI_y}(g)\ I_y = -\frac{dI_{1y}}{dB_y}(g)\ \Delta B_y \tag{15}$$

We arrive at the trim winding current settings to cancel an applied external field:

$$I_x = -\frac{\frac{dI_{1x}}{dB_x}(g)}{\frac{dI_{1x}}{dI_x}(g)}\Delta B_x \tag{16}$$

$$I_y = -\frac{\frac{dI_{1y}}{dB_y}(g)}{\frac{dI_{1y}}{dI_y}(g)}\Delta B_y \tag{17}$$

After the calibrations have been performed, this procedure should be tested by applying a range of external fields and setting the current in the trim windings to cancel the effect on the field integrals from the applied fields. Measure the field integrals to verify that the values are the same as with zero applied field.

7 Measurements

In this section we first demonstrate that the small changes in the background field and the small field from the corrector coils cause a linear change in the field integrals. We then give the measured responses of the field integrals as a function of gap. Finally, we give the calibration values.

As a check on the Helmholtz coil measurements, we calculate the field integral response at large gap where there is minimal influence from the steel poles. At large gap, when the Helmholtz coil makes a field change dB_x, the field integral change should be $dI_{1x} = dB_x L$, where L is the length of the stretched wire. So $dI_{1x}/dB_x = L$. The length of the stretched wire is approximately $L = 3.6$ m. A similar relation applies for dI_{1y}. At large gaps, the external field response functions should have the following values

$$\frac{dI_{1x}}{dB_x} = 360\ \mu\text{Tm/G} \tag{18}$$

$$\frac{dI_{1y}}{dB_y} = 360\ \mu\text{Tm/G} \tag{19}$$

A complication is the effect of the steel frame of the HE-SXR undulator. This will affect the Helmholtz coil B_y field, so a modest deviation from these values is acceptable for the HE-SXR undulator.

For a check on the beam pipe corrector measurements, we use the simulated fields with no steel poles. As given above, the simulation with no steel poles gives for the HE-SXR beam pipe corrector

$$\frac{dB_x}{dI_x} = 0.340\ \text{G/A} \tag{20}$$

$$\frac{dB_y}{dI_y} = 0.986\ \text{G/A} \tag{21}$$

The change in the field integral should be $dI_{1x} = dB_x L$, where $L = 3.6$ m is the length of the stretched wire. A similar relation applies for dI_{1y}. For the HE-SXR undulators, at large gap we have

$$\frac{dI_{1x}}{dI_x} = 122\ \mu\text{Tm/A} \tag{22}$$

$$\frac{dI_{1y}}{dI_y} = 355\ \mu\text{Tm/A} \tag{23}$$

The steel frame of the HE-SXR undulator is far enough from the beam pipe that it should not affect these results.

7.1 Linearity Of Response

When the Helmholtz coil applies an external field to the undulators, the measured field integrals change in a linear way. As an example, consider figure 21 which shows the response at 16 mm gap to the applied field. A line is fit to the measured points and the slope of the line is the response parameter dI_{1y}/dB_y at 16 mm gap.

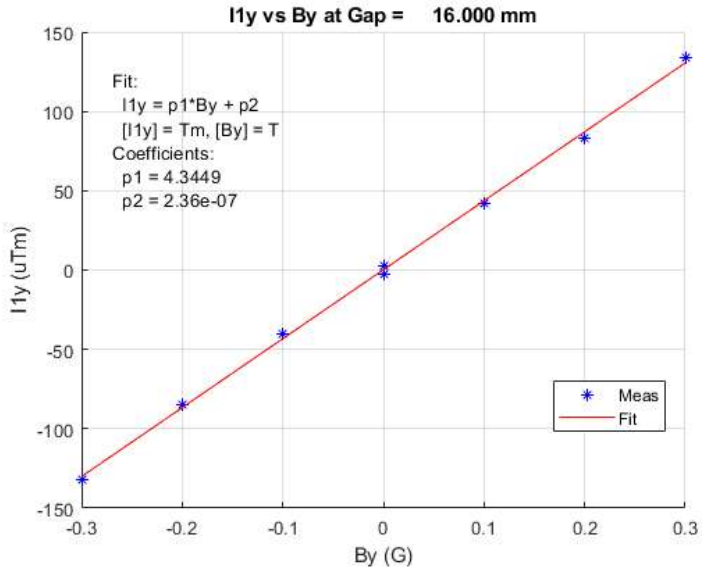

Figure 21: The measured field integral I_{1y} changes in a linear way with applied field B_y from the Helmholtz coil.

When the beam pipe corrector is energized, the measured field integrals change in a linear way with current in the coil. As an example, consider figure 22 which shows the response at 16 mm gap to the applied current. A line is fit to the measured points and the slope of the line is the response parameter dI_{1y}/dI_y at 16 mm gap.

7.2 Measured Response To An Applied Field

The Helmholtz coil was set up around HE-SXU-000 and external fields were applied. The field integrals were measured with different applied fields and the response functions dI_{1x}/dB_x and dI_{1y}/dB_y were measured at a number of undulator gaps according to the test plan given above. Figure 23 shows the measured response function dI_{1x}/dB_x as a function of gap. Also shown are the spline points and spline fit to the measurements. The measurements at large gap go roughly to the predicted result of $dI_{1x}/dB_x = 360$ μTm/G. The geometry of the steel frame should not have a large effect on B_x at large gap. At small gap, the steel poles shunt B_x around the gap and the field integral I_{1x} goes to zero.

Figure 24 shows the measured response function dI_{1y}/dB_y as a function of gap. Also shown are the spline points and spline fit to the measurements. The measurements at large gap do not go to the predicted result of $dI_{1y}/dB_y = 360$ μTm/G due to the steel frame. This was also seen in the previous calibrations and tests were performed to verify that the steel frame is responsible (see LCLS-TN-20-2). At smaller gaps, the vertical B_y field is drawn into the steel poles and through the gap amplifying the external B_y. There is less saturation at small gap due to the pole chamfers, so dI_{1y}/dB_y does not drop off as seen in the previous calibration described in LCLS-TN-20-2.

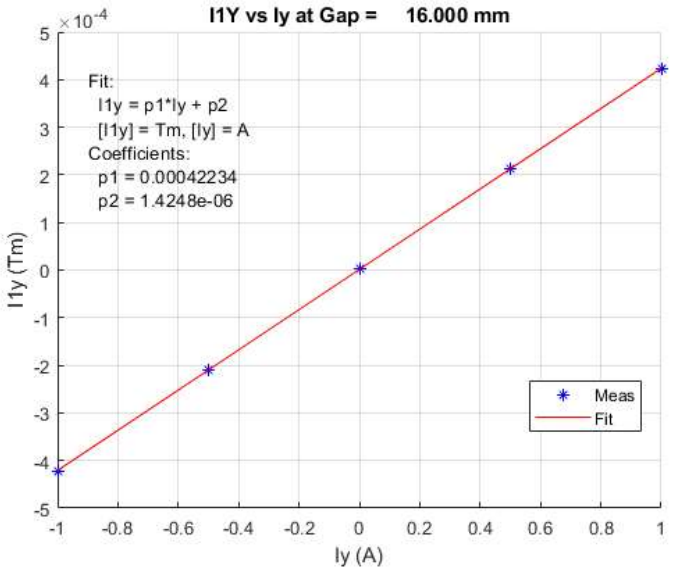

Figure 22: The measured field integral I_{1y} changes in a linear way with applied beam pipe corrector current I_y.

7.3 Measured Response To The Beam Pipe Corrector

A beam pipe with correction coils was set up in HE-SXU-000. The field integrals were measured with different coil currents and the response functions dI_{1x}/dI_x and dI_{1y}/dI_y were calculated at a number of undulator gaps according to the test plan given above.

Figure 25 shows the measured response function dI_{1x}/dI_x as a function of gap. Also shown are the spline points and spline fit to the measurements. The measurements at large gap approximately go to the expected result of $dI_{1x}/dI_x = 122$ μTm/A. The shape of the curve at small gap agrees with the result from the image current model discussed above.

Figure 26 shows the measured response function dI_{1y}/dI_y as a function of gap. Also shown are the spline points and spline fit to the measurements. The measurements at large gap approximately go to the expected result of $dI_{1y}/dI_y = 355$ μTm/A. At small gap, in the model the image currents all add enhancing the field. The measurements and the model are consistent.

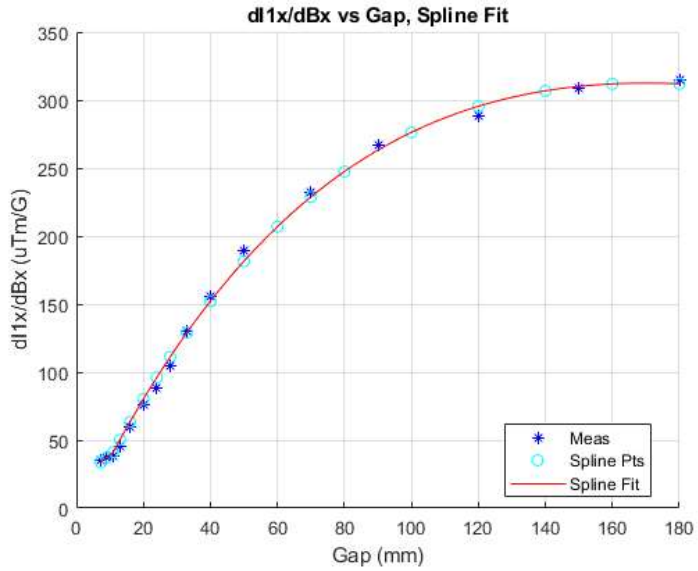

Figure 23: Response function dI_{1x}/dB_x as a function of gap.

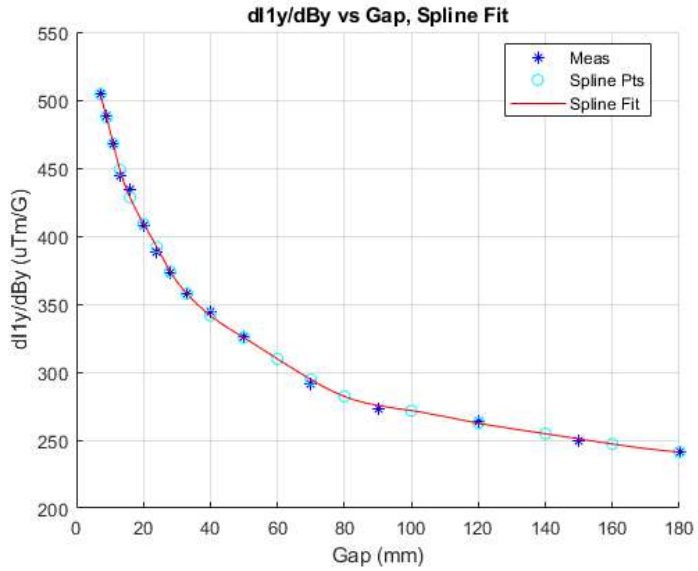

Figure 24: Response function dI_{1y}/dB_y as a function of gap.

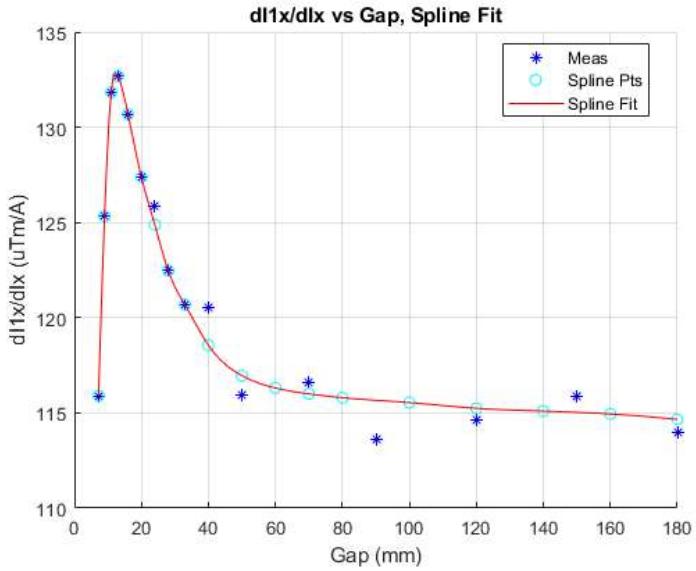

Figure 25: Response function dI_{1x}/dI_x as a function of gap.

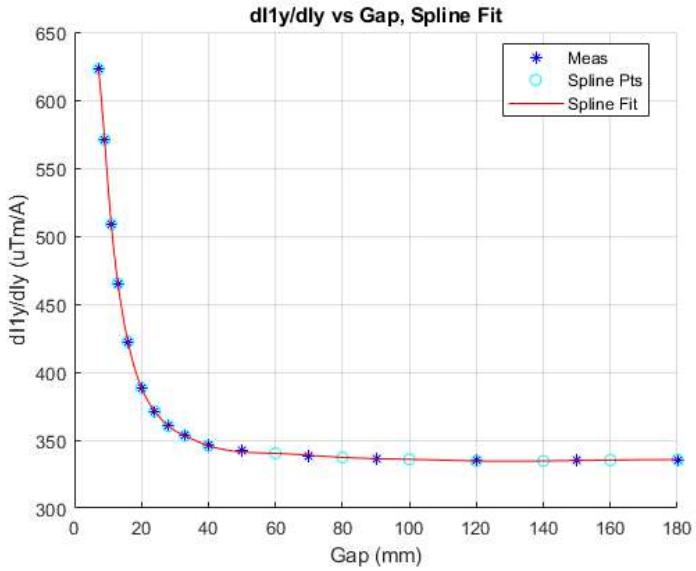

Figure 26: Response function dI_{1y}/dI_y as a function of gap.

7.4 Calibration

The external field calibration factors dI_x/dB_x and dI_y/dB_y are calculated from the results given above. They were measured on HE-SXU-000, but we assume they are the same for all HE-SXR undulators because of the similarity of the devices. A set of gaps are chosen and the spline fits give dI_{1x}/dB_x, dI_{1y}/dB_y, dI_{1x}/dI_x and dI_{1y}/dI_y at the chosen gaps. The negative of the ratios give the calibration factors dI_x/dB_x and dI_y/dB_y where the currents I_x and I_y now mean the currents used to correct external field differences. The calibration factors as a function of gap are put into spline files. For any gap, when the calibration factor from the spline is multiplied by the difference in external field between the tunnel and the laboratory ΔB_x or ΔB_y, one gets the beam pipe corrector current required to straighten the beam trajectory.

$$I_x = \frac{dI_x}{dB_x}\Delta B_x \tag{24}$$

$$I_y = \frac{dI_y}{dB_y}\Delta B_y \tag{25}$$

The calibration factors for the HE-SXR undulators are given in figures 27 and 28.

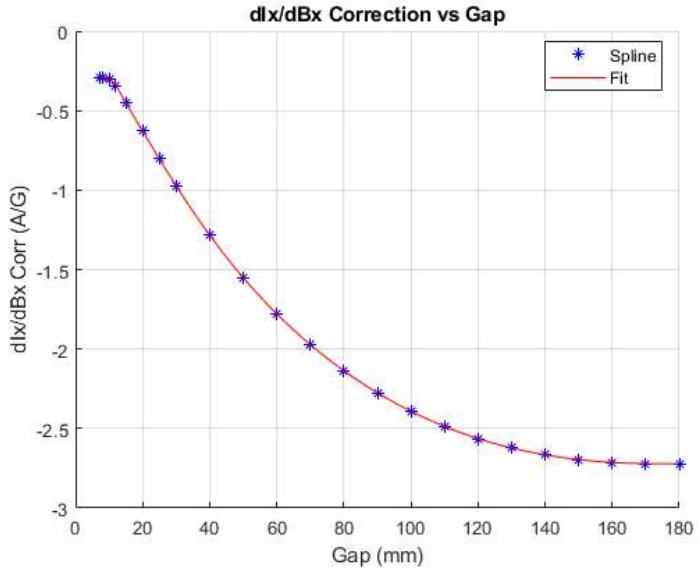

Figure 27: Calibration factor dI_x/dB_x for the HE-SXR undulators.

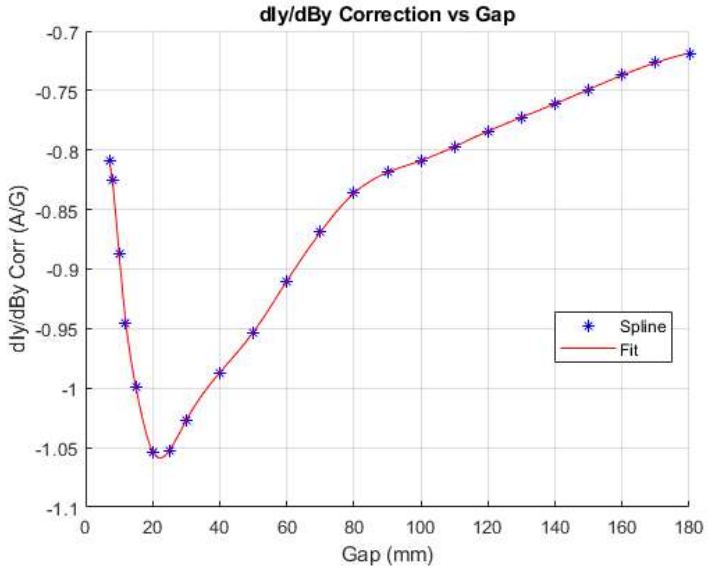

Figure 28: Calibration factor dI_y/dB_y for the HE-SXR undulators.

7.4.1 Calibration Checks

After the calibrations were done, a series of checks was made. At different gaps, the field integrals were measured with no current in either the Helmholtz coil or the beam pipe correctors. These measurements were combined with the measurements during the calibration with no current in either the Helmholtz coil or the beam pipe correctors in order to determine the background field integrals. To test the calibration, we applied an external field from the Helmholtz coil. Using the calibration data, we applied the current in the beam pipe windings calculated to cancel the effect of the external field. We then measured the field integrals again with both the Helmholtz coil field and beam pipe correctors on. We obtained the same field integrals as when no current was in the Helmholtz coil or the beam pipe correctors at the 10 μTm level. With these checks we verified the accuracy of the calibration factors.

As an example, consider checks of the beam pipe corrector calibration using background fields from cells 32, 42, and 44 in the tunnel. A fluxgate probe was used to measure the background fields in the cells, and also the background fields at the measurement bench in the MMF. The field difference for cell 32 is $\Delta B_x = 0.10$ G, $\Delta B_y = -0.11$ G. The field difference for cell 42 is $\Delta B_x = -0.10$ G, $\Delta B_y = 0.06$ G. The field difference for cell 44 is $\Delta B_x = -0.15$ G, $\Delta B_y = -0.16$ G. Using these cells, a range of background fields was tested. We then generated these field differences relative to the MMF background field using the Helmholtz coil. For example, the Helmholtz coil currents for cell 32 were $I_x = 33.6$ A, $I_y = -37.4$ A. Over the 3.4 m long undulator and with no field amplification from the steel poles, the generated external field integrals were $\Delta I_{1x} = 34$ μTm and $\Delta I_{1y} = -37$ μTm. At small gap, ΔI_{1y} would increase to 82 μTm due to the amplification factor of 2.2 from the steel poles. Without correction, the difference in background fields would cause field integrals which exceed the field integral tolerance. As part of the calibration, spline files were generated for each cell giving the beam pipe corrector settings as a function of undulator gap for the given measured field differences. We used the spline files to set the beam pipe corrector currents. We then measured the field integrals as a function of gap and compared to the field integrals with no current in the Helmholtz coil or in the beam pipe corrector. Figure 29 shows I_{1x} for the test and for the background measurements. The beam pipe correctors compensated the external field. The results for I_{1y} are shown in figure 30. The error in the correction is below 10 μTm, which is significantly below the 50 μTm tolerance.

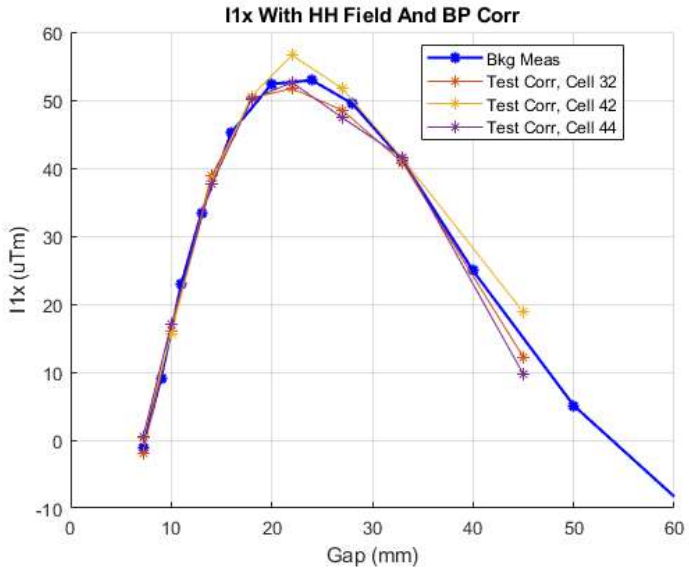

Figure 29: I_{1x} is corrected to background levels by the beam pipe corrector when an external field is applied.

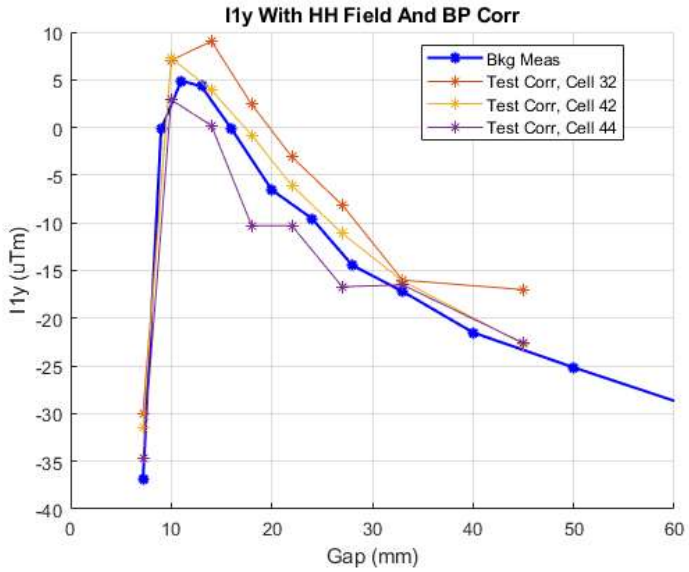

Figure 30: I_{1y} is corrected near background levels by the beam pipe corrector when an external field is applied.

8 Summary

The beam pipe corrector calibration to correct external magnetic fields was presented. For any undulator gap, a spline fit to the calibration gives a parameter dI/dB, which is multiplied by the difference in magnetic fields between the tunnel and the laboratory to give the beam pipe corrector current to correct for the field difference.

Acknowledgements

We are grateful to Heinz-Dieter Nuhn for many discussions about this work.